A Turbulent Mixing Length Formulation for Non-Newtonian Power Law Fluids

ARTHUR M. HECHT*
General Electric Company, Philadelphia, Pa.

The velocity profiles for non-Newtonian power law fluids are investigated and the friction factor is determined for pipe flow at high Reynolds numbers. The total shear stress is equated to the sum of the laminar power law stress and the turbulent stress, the latter based on the Prandtl mixing length. The analysis uses Van Driests' model for variation of the mixing length near the wall to yield a continuous velocity and shear stress distribution for incompressible turbulent flow. The shear stress equation is solved in terms of generalized parameters to yield velocity profiles near the wall as a function of the non-Newtonian fluid index N. Pipe flow is investigated by integrating the flow equation over the pipe radius, and the friction factor is determined. It is found that the theory agrees well with the results of previous analysis and experiment, while anomalous experimental results are matched using the proper values of power law index and mixing length parameter.

Nomenclature

A = distance from wall where influence of wall damping on κ becomes negligible
A_+ = $A\tau_w^{(2-N)/2N}\rho^{1/2}/a^{1/N}$
A_* = $A_+\kappa$
a = non-Newtonian property defined by Eq. (1)
B = constant in law of wall
$B_*(N)$ = defined by Eq. (39)
D = pipe diameter
f = friction factor, $2\tau_w/\rho V^2$
ℓ = mixing length
N = power law index
R = tube radius
Re_N = $(2R)^N V^{2-N}\rho/a$
Re_G = $8Re_N/(6 + 2/N)^N$
R_w = $2RV\rho/\tau_w{}^{(N-1)/N}a^{1/N}$
u = fluid velocity
u_+ = u/v_*
u_* = $u_+\kappa$
V = mean fluid velocity of flow
v_* = friction velocity, $(\tau_w/\rho)^{1/2}$
y = distance from wall
y_+ = $y^N\tau_w{}^{(2-N)/2}\rho^{N/2}/a$, $y^N v_*{}^{2-N}\rho/a$
y_* = $y_+{}^{1/N}\kappa$
κ = mixing length constant in wall region
λ = mixing length constant in turbulent core
μ = molecular viscosity
ρ = fluid density
τ = local shear stress

Subscripts

c = turbulent core
L = laminar sublayer
T = transition zone
w = at the wall
$*$ = denotes parameter independent of κ
$+$ = power law fluid parameter

Introduction

THE characteristics and behavior of non-Newtonian fluids has been of interest to the chemical processing industry for many years. Recently, the drag-reducing qualities of polymer additives in the boundary layer of underwater and surface vehicles has given added impetus toward determining the underlying mechanisms of drag reduction. There have been numerous investigations, both analytical and experimental, of the behavior of non-Newtonian turbulent flow. Dodge and Metzner[1] performed an extensive investigation into the causes of drag reduction in non-Newtonian systems, and their work marked a departure point for investigations of this nature in their proposed definitions of the nondimensional profile and friction factor parameters. In investigating the velocity profiles and heat transfer in pseudoplastic fluids, Clapp[2] extended the unified approach of Prandtl.[3]

During subsequent analytical and experimental investigations of non-Newtonian behavior, divergent views have developed concerning whether the Newtonian mixing length parameter remains a constant equal to 0.4 in the flow of viscoelastic fluids, or whether it decreases under certain circumstances. Wells,[4] Lowe,[5] Giles[6] and Van Driest,[7] among others, report reductions in κ, while Elata et al.,[8] Meyer,[9] and Ernst,[10] consider κ as constant and correlate the data in terms of a velocity displacement near the wall.

The present approach to the problem, integration of the shear stress equation using a finite difference computer technique, is based on the work of Van Driest[11] and Spalding and Patankar[12] (for example) who solved the Newtonian turbulent velocity profiles in the near-wall region in a similar fashion using computer calculated profiles. This eliminates the requirement of making excessively simplified assumptions to model the flow. κ is treated as a variable in this context to determine whether this approach can rationalize the conflicting observations mentioned above.

Analysis

The laminar shear stress of a large class of non-Newtonian fluids may be described over a wide range of shear rates by the power-law relation

$$\tau = a(du/dy)^N \tag{1}$$

where N is the power law index and a is a fluid property, which reduces to the molecular viscosity for $N = 1$.

Prandtl[3] postulated that the total shear stress in a turbulent Newtonian fluid could be written as the sum of the laminar molecular shear and the turbulent shear stress contribution

$$\tau = \mu(du/dy) + \rho\ell^2(du/dy)^2 \tag{2}$$

Clapp[2] modified Eq. (2) to include the effect of non-Newto-

Received October 2, 1970; revision received April 28, 1971.
Index category: Boundary Layers and Convective Heat Transfer—Turbulent.
* Engineer, Heat Transfer Technology, Re-Entry and Environmental Systems Division. Member AIAA.

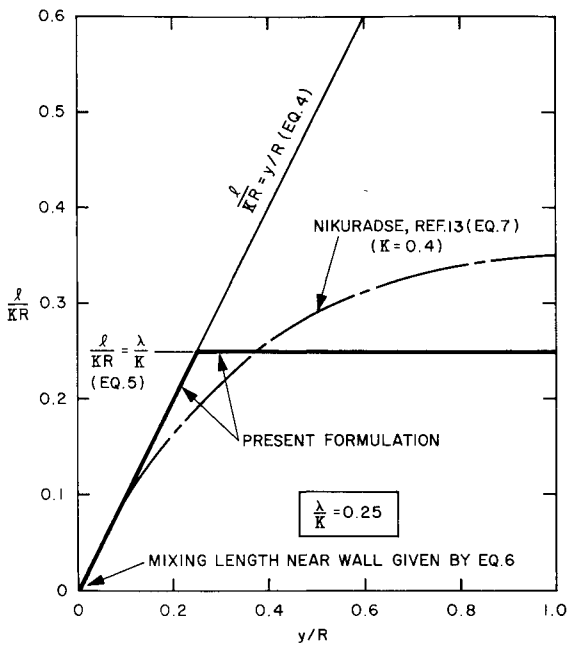

Fig. 1 Mixing length formulation as a function of pipe radius.

nian power law shear by replacing the Newtonian molecular contribution by the stress in Eq. (1)

$$\tau = a(du/dy)^N + \rho\ell^2(du/dy)^2 \tag{3}$$

The turbulent stress was assumed to be independent of the non-Newtonian fluid characteristics, and is based solely on momentum exchange considerations.

The local shear stress near the wall is very nearly equal to the wall value for zero mass injection and pressure gradient. In the outer part of the flow, the shear stress must reach zero at the pipe centerline or at the edge of the boundary layer. Since the laminar sublayer, the transition region, and the law of the wall regime are usually small compared to the turbulent core, a constant shear stress equal to that at the wall will be assumed in this region. When consideration is given to regions far from the wall, the linear pipe flow variation of τ will be used.

The mixing length adopted in the solution of Eq. (3) is the key to the derivation of an unified approach to the solution of continuous velocity profiles. Separating the flow into four zones, the laminar sublayer is $0 \leq y \leq y_L$; the transition zone is $y_L \leq y \leq y_T$; the law of the wall regime is $y_T \leq y \leq y_c$; and the turbulent core is $y_c \leq y \leq R$.

In the wall region, the mixing length is usually assumed proportional to distance from the wall

$$\ell = \kappa y \tag{4}$$

while in the turbulent core the value of ℓ is assumed proportional to a characteristic length of the flow, here taken as R

$$\ell = \lambda R \tag{5}$$

κ, the universal mixing constant for Newtonian fluids, usually taken equal to 0.4, cannot be assumed to be a universal constant for non-Newtonian fluids, since elasticity effects may produce a reduction in κ for pseudoplastic flow. In Fig. 1, the nondimensional mixing length $\ell/\kappa R$ is plotted vs y/R, where the ratio λ/κ is set equal to 0.25. The basic nature of this ratio in non-Newtonian flow suggests investigations into variation of λ/κ with viscoelastic effects.

Van Driest[11] modified Eq. (4) near the wall to account for damping of the turbulent eddies by the viscous sublayer. The damping factor adopted by Van Driest then produced a mixing length model near the wall which provided a smooth variation in the mixing length from the wall to the region where the wall influence became negligible. Thus

$$\ell = \kappa y[1 - \exp(-y/A)] \tag{6}$$

where A is a measure of the distance to the end of wall effect on damping. The assumption $\ell = \lambda R$ is usually made in wake or jet flow, and is justifiable on the grounds that we are dealing with the turbulent core. The value of λ found experimentally for Newtonian fluid is usually nearly 0.10. It is possible, of course, to use the variation of mixing length over the pipe diameter given by Nikuradse[13]

$$\ell/R = 0.14 - 0.08[1 - (y/R)^2] - 0.06[1 - (y/R)] \tag{7}$$

Equation (5) is used to simplify the approach. It will be shown that the results justify this assumption, although analysis of data in this region could possibly lead to further refinement and improvement of the results at lower values of Reynolds number.

The parameters are nondimensionalized using appropriate reference quantities usually associated with non-Newtonian power law fluid flow

$$u_+ = u/v_* \tag{8}$$

$$y_+ = y^N v_*^{2-N}\rho/a \tag{9}$$

$$\ell_+ = \ell^N v_*^{2-N}\rho/a \tag{10}$$

Wells,[4] using an analysis based on an analysis of Van Driest and Blumer[14] for the stability limit of the laminar sublayer, postulated that

$$\kappa y_{+L}^{1/N} = \text{const} \equiv y_{*L} \tag{11}$$

which indicated that if κ decreased y_{+L} should increase. The parameter given by Eq. (11), therefore, appears to be a better choice of a universal non-Newtonian parameter than y_+ given by Eq. (9). The basic parameters used in the solution of Eq. (3) become

$$u_* = u\kappa/v_* \tag{12}$$

$$y_* = y\tau_w^{(2-N)/2N}\rho^{1/2}\kappa/a^{1/N} \tag{13}$$

$$\ell_* = l\tau_w^{(2-N)/2N}\rho^{1/2}/a^{1/N} \tag{14}$$

Eq. (3) becomes

$$(1 - y_*/R_*) = (du_*/dy_*)^N + l_*^2(du_*/dy_*)^2 \tag{15}$$

where

$$R_* = R\tau_w^{(2-N)/2N}\rho^{1/2}\kappa/a^{1/N} \tag{16}$$

and

$$\ell_* = y_*[1 - \exp(-y_*/A_*)] \tag{17}$$

in the region $0 \leq y_* \leq y_{*c}$, while

$$\ell_* = (\lambda/\kappa)R_* \tag{18}$$

for $y_{*c} \leq y_* \leq R_*$.

For plane flows or for investigations near the wall, the left side of Eq. (12) is set equal to 1.0 and Eq. (17) is used for the mixing length

$$1 = (du_*/dy_*)^N + y_*^2[1 - \exp(-y_*/A_*)]^2(du_*/dy_*)^2 \tag{19}$$

The boundary between the wall region where ℓ_* is proportional to y_* and the core region where $\ell_* = (\lambda/K)R_*$ is defined by

$$y_{*c} = (\lambda/\kappa)R_* \tag{20}$$

If κ is a variable for elastic fluids depending on the polymer concentration and shear stresses it is reasonable to expect that λ will also be variable. Also, because of considerations to be discussed shortly lead to the conclusion that the turbulent fluctuations are suppressed in the core for very small values of

N, λ appears to approach zero as N approaches zero. κ may also be a function of N, although this is not clear at the present time. κ is assumed independent of N until further information is available.

The values of A_* used in Eq. (17) may be derived from the same argument used to derive y_{*L} and y_{*c}. Van Driest found that a value of $A_+ = 26$ gave the best results for the damping factor in Newtonian fluid flow, with $\kappa = 0.4$. Therefore since $A_* = \kappa A_+$, $A_* = 10.4$ will be used throughout this analysis for variable N and κ.

The parameter R_* may be related to the non-Newtonian Reynolds number Re_N using the definition of the friction factor and the friction velocity

$$R_* = \tfrac{1}{2}\kappa Re_N^{1/N}(V/v_*)^{(N-2)/N} \tag{21}$$

where

$$V/v_* = (f/2)^{-1/2} \tag{22}$$

The mean linear velocity of flow, V, is defined by

$$\pi R^2 V = 2\pi \int_0^R u(R - y)dy \tag{23}$$

In nondimensional form this becomes

$$V_* = \frac{V\kappa}{v_*} = 2\int_0^1 u_* \left(1 - \frac{y_*}{R_*}\right) d\left(\frac{y_*}{R_*}\right) \tag{24}$$

From Eq. (21), the generalized relationship between V_* and R_* is

$$(2R_*)^N V_*^{2-N} = \kappa^2 Re_N \tag{25}$$

Approximate Solutions

Certain interesting properties of Eqs. (15) and (19) are evident if limiting values of solutions are investigated. Five cases suggest themselves:

1) Laminar sublayer:

$$y_* \ll R_* \qquad y_* < y_{*L} \qquad \ell_* \cong 0$$
$$u_* = y_* \tag{26}$$

2) Law of the wall regime:

$$y_{*T} < y_* \ll R_* \qquad \ell_* = y_*$$
$$u_* = \ln y_* + B_* \tag{27}$$

Note that this approach fails to account for the effect of non-Newtonian shear, since the molecular shear term has been neglected.

3) Turbulent core:

$$y_* > y_{*c} \qquad \ell_* = (\lambda/\kappa)R_*$$
$$(u_{*m} - u_*)/u_{*m} = (1 - y_*/R_*)^{3/2} \tag{28}$$

where u_{*m} is the centerline velocity parameter

$$u_{*m} = 2\kappa/3\lambda \tag{29}$$

From experimental and theoretical considerations Dodge and Metzner[1] found

$$(u_m - V)/v_* = 3.686N^{0.25} \tag{30}$$

or

$$u_{*m} - V_* = 3.686\kappa N^{0.25} \tag{31}$$

This equation, along with the limiting cases of fully laminar flow and $N \cong 0$, provides the means to evaluate λ.

4) Fully laminar flow: Eq. (15) then becomes

$$du_*/dy_* = (1 - y_*/R_*)^{1/N} \tag{32}$$

which has the solution

$$u_* = (3N + 1)/(N + 1)V_*[1 - (1 - y_*/R_*)^{(N+1)/N}] \tag{33}$$

where Eq. (24) is used to find $u_{*m} = V_*(3N + 1)/(N + 1)$. Equations (24, 25, and 33) along with Eq. (22) written in the form

$$f = 2\kappa^2/V_*^2 \tag{34}$$

provide the friction factor in terms of the Reynolds number:

$$f = 16/\{Re_N[8(N/(6N + 2))^N]\} \tag{35}$$

and the generalized non-Newtonian Reynolds number is

$$Re_G = 8Re_N[N/(6N + 2)]^N \tag{36}$$

5) $N \to 0$.

For very small values of N, the flow velocity acquires a flat profile across essentially the entire pipe diameter. The turbulent fluctuations are suppressed almost completely away from the wall, while the laminar sublayer thickness increases. The result is a flat velocity profile flow for $N = 0$, with $u_{*m} = V_*$. For small values of N in turbulent flow therefore, we shall adopt the variation of u_{*m} with N obtained for laminar flow, namely

$$u_{*m} \cong [(3N + 1)/(N + 1)]V_* \tag{37}$$

Using the above expression in Eq. (31), and substituting u_{*m} given by Eq. (29), the turbulent core mixing length constant becomes

$$\lambda = 0.09[4N^{0.75}/(3N + 1)] \tag{38}$$

which indicates, as expected, that λ goes to zero as N approaches zero. Also, for $N = 1$, Eq. (38) yields a value $\lambda = 0.09$, which matches the experimentally measured values of λ in the turbulent case for Newtonian fluids quite well. This suggests that Eq. (38) can be used to evaluate λ over the entire range of N for pseudoplastic fluids.

Friction Factor

The friction factor is determined by integrating Eq. (15) over the tube radius. V_* is evaluated simultaneously using Eq. (24). The parameter R_* is chosen arbitrarily; then using Eqs. (25, 34, and 36) the values of Re_N, f, and Re_G are found, respectively. Equation (38) is used to define λ. The results of this calculation are discussed in the next section where the velocity profiles and friction factors calculated with the present method are compared to previous work and experimental measurements.

Near-Wall Velocity Profiles

Equation 19 has been integrated for the near-wall region, and u_* vs y_* is plotted in Fig. 2 for various values of N. The

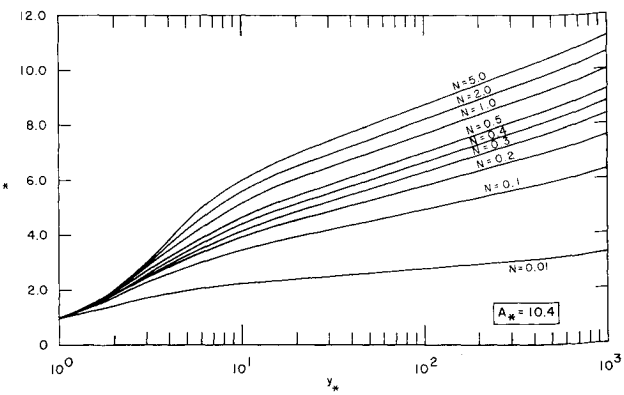

Fig. 2 Near-wall generalized velocity profiles as a function of the power-law index.

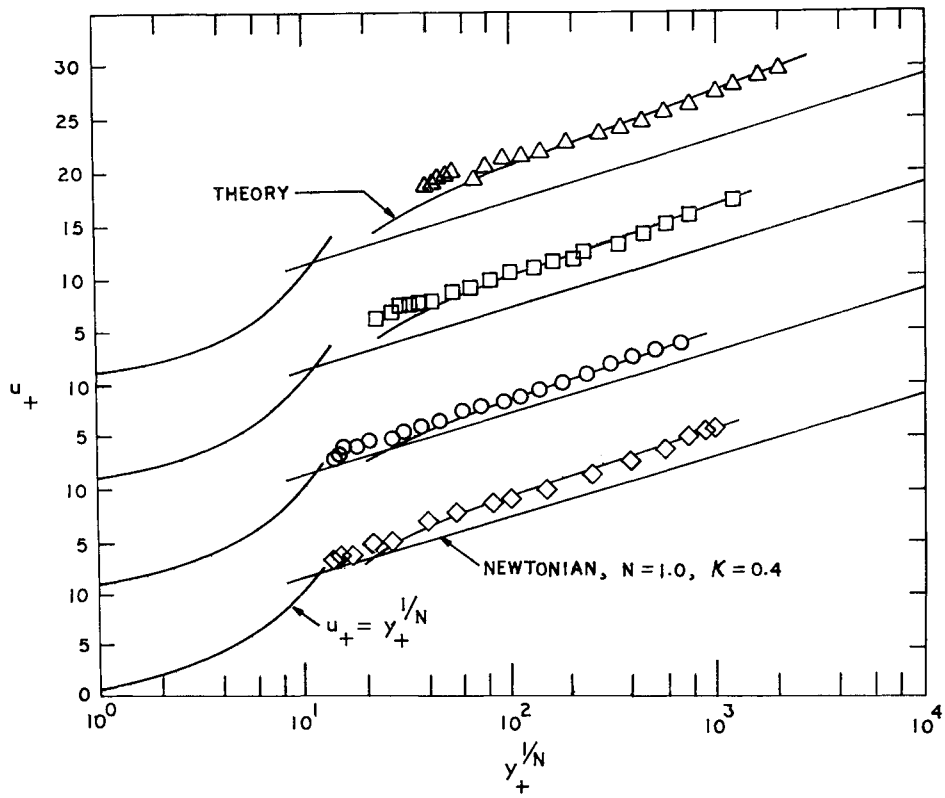

Fig. 3 Comparison of calculated velocity profiles with experimental results of Ernst.

mixing length is assumed given by Eq. (17). The solution provides law of the wall profiles of the form

$$u_+ = A_*(N) \ln y_* + B_*(N) \tag{39}$$

where A_* (1) = 1.0. Translated into the usual variables associated with this region

$$u_+ = \frac{A_N}{\kappa N} \ln y_+ + B_N \tag{40}$$

where

$$B_N = \frac{B_*(N)}{\kappa} + \frac{A_*(N)}{\kappa} \ln \kappa \tag{41}$$

For N less than 0.3, the profiles in the u_*, y_* coordinate system appear to approach $u_* = 1.0$. For $N = 1.0$, $\kappa = 0.4$, Fig. 2 yields a value of $A_*(1) = 1.0$, $B_*(1) = 3.13$, such that Eq. (40) can be written

$$u_+ = 2.5 \ln y_+ + 5.5 \tag{42}$$

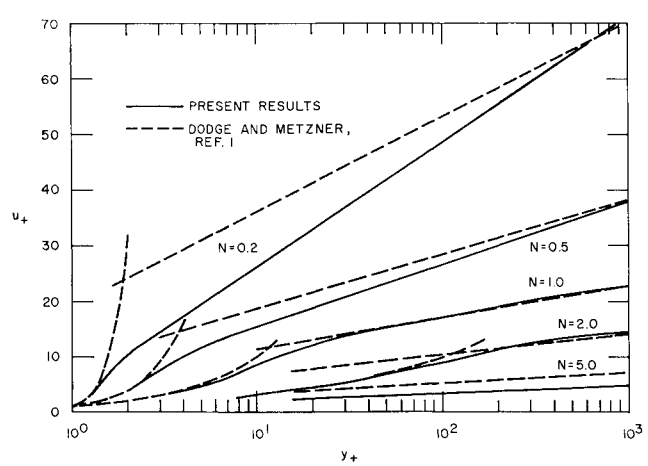

Fig. 4 Comparison of near-wall velocity profiles with results of Dodge and Metzner.

which is recognized as the universal velocity distribution for smooth walls for large Reynolds numbers in Newtonian fluid flow.

Comparison with Previous Results

Correlation of the velocity profile based on a velocity displacement, as presented by Meyer[9] and Ernst,[10] are based on observed velocity profiles and the assumption of a parallel displacement of the profile in the law of the wall regime. The present theory has been applied to the experimental data of Ernst[10] by fitting data using a reduced value of κ for the reported value of Reynolds number. Figure 3 presents the results of this procedure. $N = 0.9$ was used for the calculations, while the experimental value varied from 0.9–0.93. The experimental velocity profiles are matched well in the region of reliable measurements. The correlations of Refs. 9 and 10, based on a velocity displacement dependent upon the friction velocity exceeding a threshold value v_{*cr}, and the polymer concentration, can also be interpreted as the result of the mixing length parameter κ varying as a result of the friction velocity exceeding this threshold value. The rate of decrease of κ would also be dependent upon concentration.

Figure 4 is a comparison of the present velocity profiles with the results of Dodge and Metzner. The agreement is excellent for N ranging near or greater than 1.0, with an acceptable comparison for $N = 0.5$. For $N = 0.2$, (where Dodge and Metzner report extrapolated results) the present

Table 1 Identification of data[a] and theoretical parameters of Fig. 3

Symbol	R_w	Tube diam, in.	κ^b	N
△	1.11×10^5	$\frac{3}{4}$	0.31	0.9
□	5.9×10^4	$\frac{3}{4}$	0.31	0.9
○	2.72×10^4	$\frac{3}{4}$	0.35	0.9
◇	6.8×10^4	$1\frac{1}{2}$	0.33	0.9

[a] Data of Ernst, Ref. 10.
[b] κ assumed to fit data.

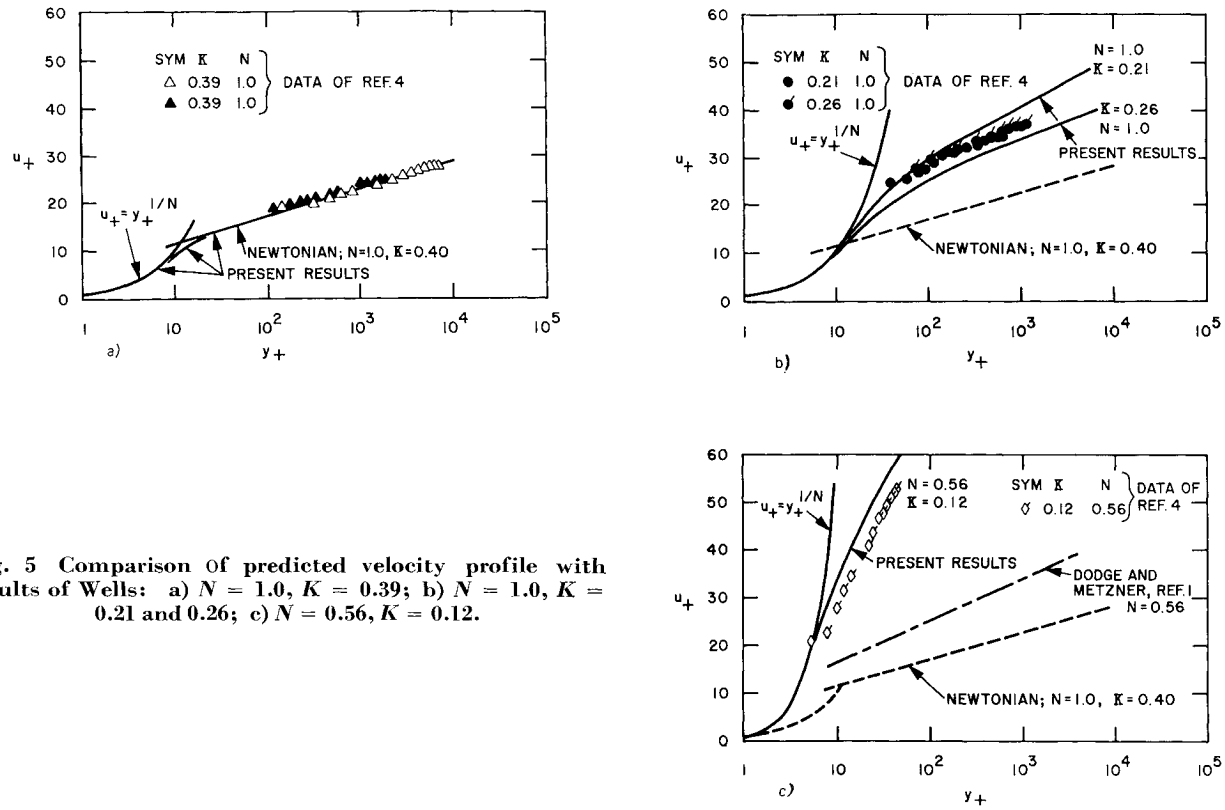

Fig. 5 Comparison of predicted velocity profile with results of Wells: a) $N = 1.0$, $K = 0.39$; b) $N = 1.0$, $K = 0.21$ and 0.26; c) $N = 0.56$, $K = 0.12$.

results indicate that the profile parameter u_+ falls below the Dodge and Metzner results.

A comparison of the present profile predictions with the turbulent pipe flow data of Wells[4] has been made to determine if the present theory could explain the anomalous results obtained. The measurements were made with very dilute aqueous solutions of guar gum (J-2P), with concentrations ranging from 0.05%–0.4% by weight, with power law indices from 1.0–0.56, respectively. Figure 4 presents a comparison between the measured velocity profiles and those calculated using Eq. (19). Even though N is in the region where very nearly parallel displacement of velocity profile would be expected, the reduction in κ produces the same effect as a decrease in N. This can be explained by examination of Eq. (40). The slope of the velocity profile is as sensitive to changes in κ as it is for change in N. The dimensionless velocity u_+ is vertically displaced due to variation in B_N as a function of N.

Three cases are presented in Fig. 5. The first case, Fig. 5a, is that of a Newtonian fluid with $N = 1.0$ and $\kappa = 0.4$. The calculated profile matches the laminar sublayer and logarithmic profile, providing a continuous variation of velocity, as would be expected, since this is the solution of Van Driest.[11] For $N = 1.0$ but for a lower value of κ ranging between 0.21 and 0.26, Fig. 5b, the data showed an almost parallel shift upward in velocity. The present results bound the measured profile indicated. For $N = 0.56$, $\kappa = 0.12$, Fig. 5c shows a comparison between the present results and the theory of Dodge and Metzner based on $\kappa = 0.4$.

Table 2 Identification of data[a] of Figs. 5 and 7

Symbol	N	κ	Fluid
○	1.0	0.21	0.05% J-2P
◺	0.81	0.28	0.10% J-2P
◣	0.81	0.14	0.10% J-2P
□	0.71	0.15	0.20% J-2P
■	0.71	0.10	0.20% J-2P
◇	0.56	0.12	0.40% J-2P

[a] Data of Wells, Ref. 4.

A comparison of the friction factor calculated by the present approach with the results of Dodge and Metzner is presented in Fig. 6. For values of the power law index between 0.4 and 2.0, the present results are in excellent agreement with those of Ref. 1 for high Reynolds number, which appear to substantiate the extrapolation of Ref. 1 beyond the available data. The discrepancy at low Reynolds number is due to the assumption in the present theory of well developed flow throughout the radius of the pipe. Prandtl's universal law of friction for smooth pipes given by

$$1/f^{1/2} = 4.0 \log [Re(f)^{1/2}] - 0.40 \qquad (43)$$

is also plotted in Fig. 6.

A comparison with the experimental friction factor measurements of Wells[4] is shown in Fig. 7. The measurements were made in the same study which reported the velocity profiles shown in Fig. 5. Four values of N are represented in Fig. 7, $N = 1.0$, 0.81, 0.71, and 0.56. The first and last of these are the values for the data of Fig. 5. The friction factor was calculated by the present method for these values of power law index and for the reported values of mixing length κ as listed in Table 2. For values of $N = 1.0$ and $N = 0.56$, the match between data and calculated results is excellent. For intermediate values of N, the match is not as good. How-

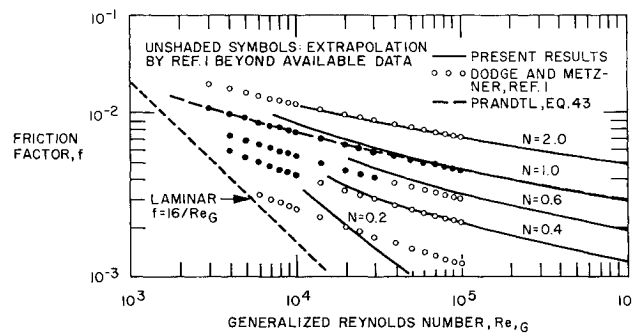

Fig. 6 Friction factor vs generalized Reynolds number and comparison with results of Dodge and Metzner; $K = 0.4$.

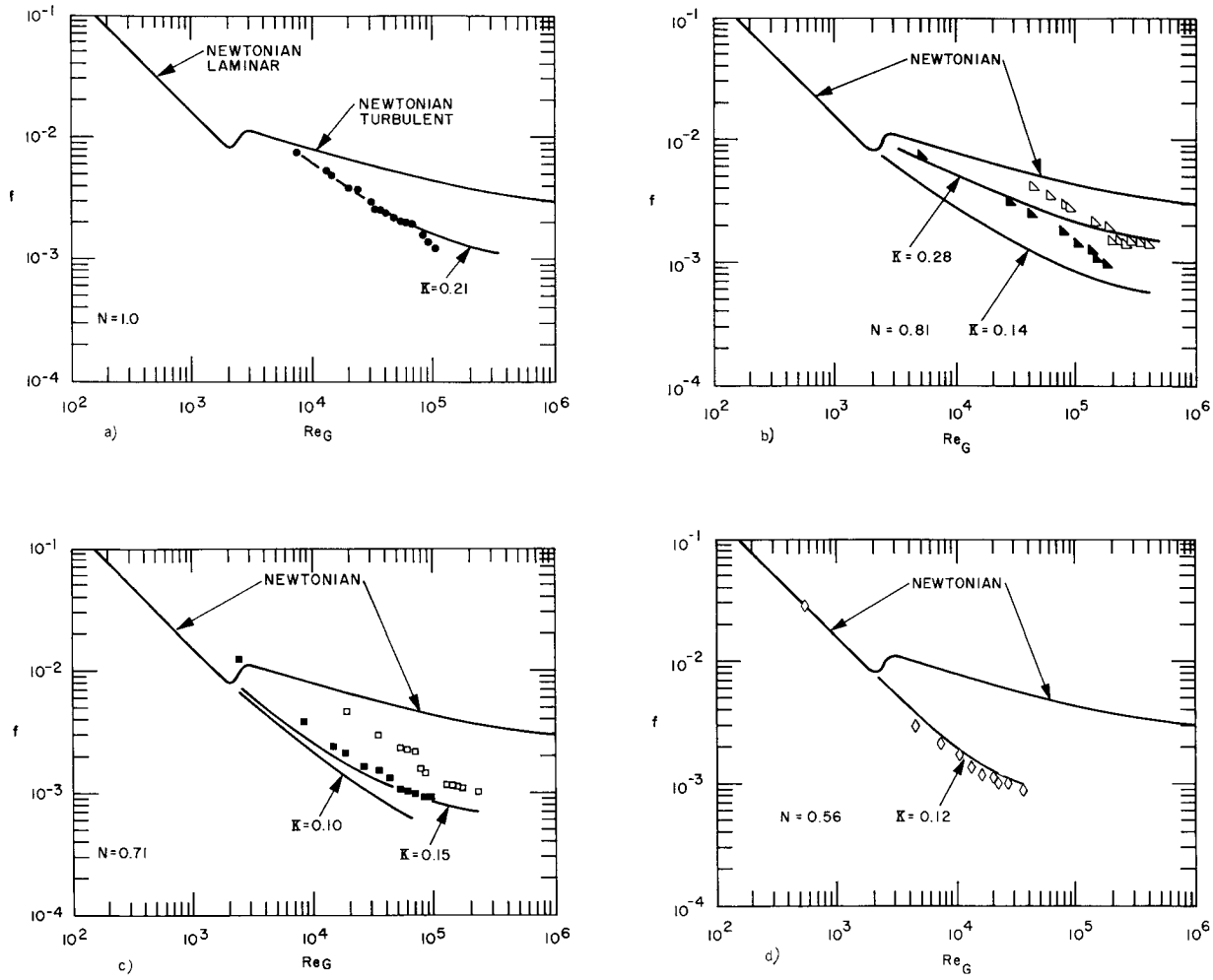

Fig. 7 Comparison of predicted friction factor with the experimental results of Wells: a) $N = 1.0$, $K = 0.21$; b) $N = 0.81$, $K = 0.28, 0.14$; c) $N = 0.71$, $K = 0.15, 0.10$; d) $N = 0.56$, $K = 0.12$.

ever, it should be noted that the correct trend is indicated as well as the correct level at high values of generalized Reynolds number.

Concluding Remarks

This analysis has examined the flow of a viscoelastic non-Newtonian power law fluids with variable mixing length. The momentum equation has been solved for a continuous velocity distribution throughout the pipe radius. This approach matches anomalous experimental velocity profiles and skin friction which could not be explained previously. In addition, the analysis suggests that a nearly parallel velocity profile shift can be produced by a reduction in the mixing length parameter. Just as in the case of a shift in the logarithmic law constant B, this reduction can be attributed to local shear stress effects and viscoelastic damping dependent upon concentration.

A possible source of velocity profile shift not dealt with in this paper is an increase in the damping factor A. Maintaining κ constant at 0.4 and increasing A produces almost precisely the calculated profiles shown in Fig. 3.

References

[1] Dodge, D. W. and Metzner, A. B., "Turbulent Flow of Non-Newtonian Systems," *American Institute of Chemical Engineers Journal*, Vol. 5, No. 2, June 1959, pp. 189–204.

[2] Clapp, R. M., "Turbulent Heat Transfer in Pseudoplastic Non-Newtonian Fluids," *International Developments in Heat Transfer*, ASME, Pt. III, Sec. A, 1961, pp. 652–661.

[3] Prandtl, L., "Neuere Ergenbnisse der Turbulenzforshung," Zeitschr Ver deut Ing., Vol. 77, 1933, p. 105.

[4] Wells, C. S., Jr., "Anomalous Turbulent Flow of Non-Newtonian Fluids," *AIAA Journal*, Vol. 3, No. 10, Oct. 1965, pp. 1800–1805.

[5] Lowe, R. J., "The Turbulent Shear Flow of Dilute Solutions of Long Chain Polymers," Masters thesis, July 1969, Univ. of Liverpool, Liverpool, England.

[6] Giles, W. B., "Projected Friction Reduction and Velocity Profiles in Large Diameter Pipes," Rept. 70-C-276, July 1970, General Electric Research and Development Center, Schenectady, N. Y.

[7] Van Driest, E. R., "Turbulent Drag Reduction of Polymer Solutions," *Journal of Hydronautics*, Vol. 4, No. 3, July 1970, pp. 120–126.

[8] Elata, C., Lehrer, J., and Kahnovitz, A., "Turbulent Shear Flow of Polymer Solutions," *Israel Journal of Technology*, Vol. 4, No. 1, 1966, pp. 87–95.

[9] Meyer, W. A., "A Correlation of the Frictional Characteristics for Turbulent Flow of Dilute Viscoelastic Non-Newtonian Fluids in Pipes, *American Institute of Chemical Engineers Journal*, Vol. 12, No. 3, May 1966, pp. 522–525.

[10] Ernst, W. D., "Turbulent Flow of an Elasticoviscous Non-Newtonian Fluid," *AIAA Journal*, Vol. 5, No. 5, May 1967, pp. 906–909.

[11] Van Driest, E. R., "On Turbulent Flow Near a Wall," *Journal of the Aeronautical Sciences*, Vol. 23, No. 11, Nov. 1956, pp. 1007–1011, 1036.

[12] Spalding, D. B. and Patankar, S. V., *Heat and Mass Transfer in Boundary Layers*, Morgan Grampian, London, 1967.

[13] Nikuradse, J., "Gesetzmässigkeiten der Turbulenten Strömung in glatten Rohren," Verein Deutscher Ingenieure-Forschungsheft, No. 356, 1932, pp. 1–36.

[14] Van Driest, E. R. and Blumer, C. B., "Boundary Layer Transition: Free-stream Turbulence and Pressure Gradient Effects," *AIAA Journal*, Vol. 1, No. 5, June 1963, pp. 1303–1306.